



Taurine reduction associated with heart dysfunction after real-world PM_{2.5} exposure in aged mice

Zenghua Qi^a, Chun Yang^a, Xiaoliang Liao^a, Yuanyuan Song^b, Lifang Zhao^c, Xiaoping Liang^d, Yuping Su^a, Zhi-Feng Chen^a, Ruijin Li^c, Chuan Dong^c, Zongwei Cai^{a,b,*}

^a Guangdong Key Laboratory of Environmental Catalysis and Health Risk Control, Guangdong-Hong Kong-Macao Joint Laboratory for Contaminants Exposure and Health, School of Environmental Science and Engineering, University of Technology, Guangzhou 510006, PR China

^b State Key Laboratory of Environmental and Biological Analysis, Department of Chemistry, Hong Kong Baptist University, Hong Kong, China

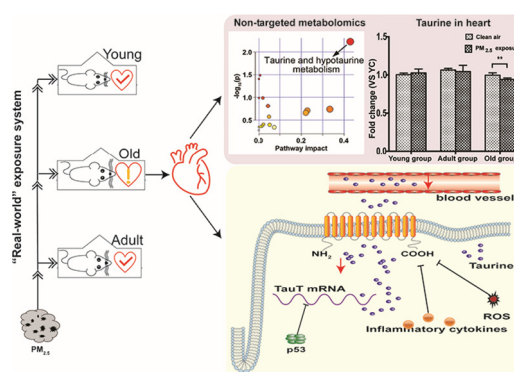
^c Institute of Environmental Science, Shanxi University, Taiyuan, China

^d School of Biomedical and Pharmaceutical Sciences, Guangdong University of Technology, Guangzhou 510006, PR China

HIGHLIGHTS

- Real-world PM_{2.5} exposure was used to study the age-related impacts on the mice heart.
- Chronic PM_{2.5} exposure mostly affected the heart function in aged mice.
- Metabolomics revealed that taurine reduction associated with heart dysfunction.
- Taurine reduction was caused by the decreased serum taurine and taurine transporter.

GRAPHICAL ABSTRACT



ARTICLE INFO

Article history:

Received 30 December 2020

Received in revised form 20 February 2021

Accepted 27 March 2021

Available online 5 April 2021

Editor: Jianmin Chen

Keywords:

PM_{2.5} exposure

Age-dependent effect

Cardiac dysfunction

Non-targeted metabolomics

Taurine

ABSTRACT

Ambient PM_{2.5} has been proved to be an independent risk factor for cardiovascular diseases; however, little information is available on the age-dependent effects of PM_{2.5} on the cardiovascular system and the underlying mechanisms following chronic exposure. In this study, multi-aged mice were exposed to PM_{2.5} via the newly developed real-ambient PM_{2.5} exposure system to investigate age-related effects on the heart after long-term exposure. First, the chemical and physical properties of PM_{2.5} used in the exposure system were analyzed. The heart rate of conscious mice was recorded, and results showed that exposure of aged mice to PM_{2.5} for 26 weeks significantly increased heart rate. Histological analysis and ELISA assays indicated that aged mice were more sensitive to PM_{2.5} exposure in terms of inducing cardiac oxidative stress and inflammation. Furthermore, untargeted metabolomics revealed that taurine was involved with the PM_{2.5}-induced cardiac dysfunction. The reduced taurine concentration in the heart was examined by LC-MS and imaging mass spectrometry; it may be due to the increased p53 expression level, ROS and inflammatory cytokines. These results emphasize the age-dependent effects of PM_{2.5} on the cardiovascular system and suggest that taurine may be the novel cardiac effect target for PM_{2.5}-induced heart dysfunction in the aged.

© 2021 Elsevier B.V. All rights reserved.

1. Introduction

PM_{2.5} is the most studied group of atmospheric particles and concerns regarding possible hazards and risks in the environment and

* Corresponding author at: Rm OE901A, Department of Chemistry, Hong Kong Baptist University, Hong Kong, China.

E-mail address: zwcai@hkbu.edu.hk (Z. Cai).

especially for human health have been raised. Despite great progress in reducing ambient $PM_{2.5}$ pollution via effective monitoring, emission control and policy actions, air quality problems are still growing in many developing nations (West et al., 2016). Taiyuan, a typical coal-powered city in China, is surrounded by mountains and is located in a semi-closed basin, making it the most contaminated area in Shanxi province, with an average concentration of $PM_{2.5}$ between 45 and 112 $\mu\text{g}\cdot\text{m}^{-3}$ (Li et al., 2015; Miao et al., 2018). The source, formation and constituents of $PM_{2.5}$ have been thoroughly studied in this city, making it particularly suitable for assessing the possible impacts of $PM_{2.5}$ on human health via “real-world” exposure (Bastiaensen et al., 2019).

The positive links between $PM_{2.5}$ exposure and cardiovascular disease (CVD) have been confirmed across countries and regions by numerous experimental and epidemiological studies. $PM_{2.5}$ air pollution, together with high systolic blood pressure, smoking, and a high-sodium diet, are considered the leading four risk factors contributing to cardiovascular morbidity and mortality (Liu et al., 2019; Zhou et al., 2019). In recent decades, adverse effects induced by $PM_{2.5}$ have been shown to differ according to personal characteristics, such as gender, age, diet and habits. Age related variations markedly affect the health risk associated with $PM_{2.5}$ pollution. Although all age groups suffer greatly as a result of $PM_{2.5}$ exposure, the elderly are particularly susceptible to severe health problems caused by poor air quality, especially those affecting the cardiovascular system (Sacks et al., 2011; Wang et al., 2015a; Pun et al., 2017). In addition, several studies have shown that mortality caused by cardiovascular disease related to atmospheric particulates ($PM_{2.5}$, PM_{10} and black carbon) in the aged is higher than that in the general population (Kan et al., 2010; Xu et al., 2013). In previous studies, oxidative stress and inflammation have been the most studied health outcomes induced by $PM_{2.5}$ exposure (Luo et al., 2007; Jia et al., 2017; Qi et al., 2020). However, the specific effects and potential mechanisms of $PM_{2.5}$ exposure on the cardiovascular system of the elderly still needed to be explored.

Taurine (2-aminoethanesulfonic acid) is the most abundant free amino acid in the heart and plays a key role in cardiovascular physiology; it has been linked to antioxidation, energy metabolism, gene expression, the excitation-contraction process, neuromodulation, the mitochondrial electron transport chain and calcium homeostasis (Schaffer and Kim, 2018). Taurine is imported into cardiac cells mainly by the taurine transporter (*SLC6A6* gene, *TAUT*), which has 12 hydrophobic transmembrane (TM) domains and delivers more than 90% of cardiac taurine (Baliou et al., 2020). Taurine has been shown to be closely related to aging and chronic $PM_{2.5}$ exposure (Dawson et al., 1996; Xu et al., 2019). However, the systematic effects of taurine, the expression of *TAUT* and their underlying mechanisms in the aged have not been previously examined following chronic $PM_{2.5}$ exposure.

Therefore, our study used a newly developed real-world $PM_{2.5}$ exposure system for $PM_{2.5}$ on C57BL/6 mice of different ages with the aim of investigating the age-related effects on the heart after chronic $PM_{2.5}$ exposure. We put special emphasis on screening novel cardiac effect targets, so as to further identify therapeutic targets against $PM_{2.5}$ -induced heart dysfunction in the aged group.

2. Materials and methods

2.1. Experimental animals

The animal protocol was approved by the Institutional Animal Care and Use Committee of Shanxi University and was consistent with the NIH Guide for the Care and Use of Laboratory Animals. Male C57BL/6 mice (young, 6-weeks old) and adult (12-months old) were purchased from the Experimental animal center of Guangzhou University of Chinese Medicine (SCXK, 2018-0034, Guangzhou, China), and aged mice (17-months old) were supplied by the Shanghai Model Organisms Center, Inc. (Shanghai, China). Mice of each age were placed in either filtered air (FA) or $PM_{2.5}$ exposure cages for 6 months. Hereafter, these are referred to as the young FA group (Young-FA), adult FA group (Adult-FA),

old FA group (Old-FA) and young $PM_{2.5}$ group (Young- $PM_{2.5}$), adult $PM_{2.5}$ group (Adult- $PM_{2.5}$), old $PM_{2.5}$ group (Old- $PM_{2.5}$) (ten mice per group). During the whole exposure period (about 6 months, from November 1, 2018 to April 19, 2019), the mice were fed commercial nutritious mouse chow (Jiangsu Xietong Pharmaceutical Bio-engineering Co., Ltd) and given access to distilled water; they were kept under a 12 h light/dark cycle.

2.2. Real-world $PM_{2.5}$ exposure

The real-ambient $PM_{2.5}$ exposure system was purchased from Suzhou Junsheng Laboratory Animal Equipment Co., Ltd. and it was used with the FA group and $PM_{2.5}$ exposure group (Fig. 1). The chambers for the FA group and the $PM_{2.5}$ exposure group had independent air intake and outlet devices connected to the system's control center. The control center takes in ambient air through a stainless-steel pipe, 2.5 m long, 10 cm diameter. Clean air and $PM_{2.5}$ particles from ambient air can be directed to the chambers containing the FA and $PM_{2.5}$ exposure groups, as appropriate, because of the filter function. The air supply system and temperature control system ensured a relatively constant temperature (23–26 °C), humidity (50–60%), and pressure (15–20 Pa). We measured $PM_{2.5}$ concentration in the chambers using a DustTrak™ II aerosol monitor (TSI Inc., USA).

2.3. Chemical analysis and morphological characterization of $PM_{2.5}$

$PM_{2.5}$ sampling sites were on the roof of the building in which the exposure experiments were conducted and the sampling period was the same as for the exposure experiment. The equipment and methods used for $PM_{2.5}$ collection followed a previous research protocol (Liao et al., 2021). Characterization of $PM_{2.5}$ constituents was performed as previously described by us (Qi et al., 2019b). Briefly, water soluble inorganic

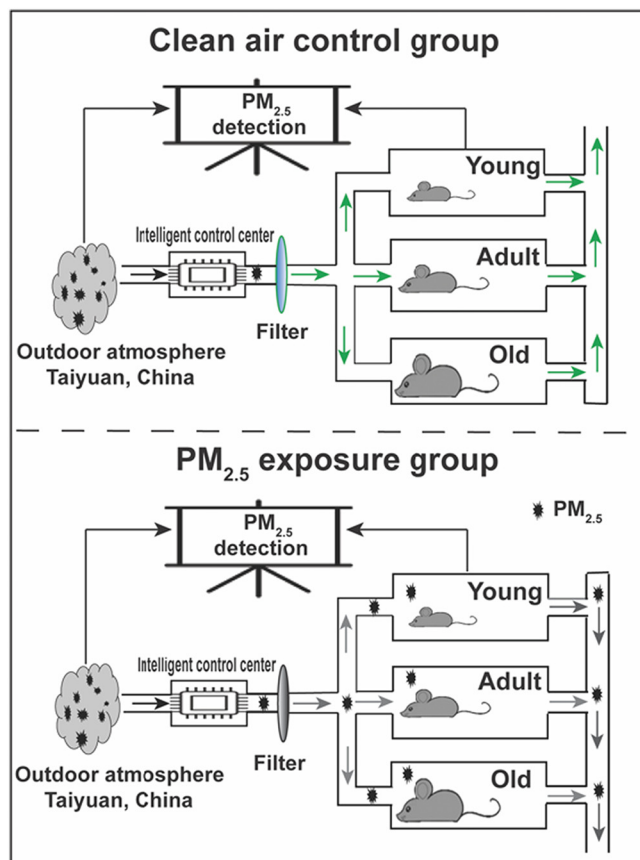


Fig. 1. Schematic diagram showing the $PM_{2.5}$ exposure system.

ions (K^+ , Na^+ , Ca^{2+} , NH_4^+ , Mg^{2+} , Cl^- , NO_3^- , SO_4^{2-}), 16 Environmental Protection Agency (EPA) PAHs, crustal elements, organic carbon (OC) and elemental carbon (EC) were determined in the collected $PM_{2.5}$ samples. Following previous research (Pozzi et al., 2003; Zhang et al., 2018), the morphology and size of $PM_{2.5}$ in suspension and filters was analyzed by scanning electron microscopy (SEM, HITACHI, SU8100, Tokyo, Japan). Prior to the analysis, the $PM_{2.5}$ filter was cut into tiny pieces and exposed to ultrasonic treatment for 20 min in dichloromethane. The suspended $PM_{2.5}$ was filtered via a nucleopore membrane to obtain well distributed and dispersed single PM samples. For detecting $PM_{2.5}$ in the filter, a piece of filter (approximately $0.3\text{ cm} \times 0.3\text{ cm}$) randomly selected from the whole $PM_{2.5}$ filter was used for the analysis. After gold plating, the morphology and size of $PM_{2.5}$ in suspension and on the filter was detected by SEM with an accelerating voltage of 3 kV.

2.4. Electrocardiogram and blood pressure recordings

Electrocardiograms (ECGs) from conscious mice were recorded non-invasively before and after $PM_{2.5}$ exposure. Briefly, mice were removed from their cages and placed on the ECGenie recording platform (Mouse Specifics, Inc., Boston, MA, USA). In order to acquire stable ECGs without external disturbance, each mouse was permitted to acclimate for at least 10 min and the test room was kept quiet during the whole recording process. Recording commenced at a sampling rate of 2000 samples/s when at least three of the mouse's paws were in full contact with the leads. At least 10 s of stable ECG recordings (more than 50 heartbeats) were analyzed by e-MOUSE software to obtain the HR of mice (Mouse Specifics, Inc., Boston, MA, USA) and the parameters were set according to previous research (Wang et al., 2015b; Heuermann et al., 2016). The blood pressure was continuously monitored and recorded with MiniTR noninvasive blood pressure analyzer (Nanjing kaerwen Biotechnology Co., Ltd., China).

2.5. Determination of reactive oxygen species and inflammatory cytokine levels in the heart

The hearts and serum were isolated from the mice harvested after exposure to the $PM_{2.5}$ treatments, with the detailed information provided in S1. The concentration levels of reactive oxygen species (ROS) and inflammatory cytokines in the heart were measured by ROS assay kit (Beyotime Institute of Biotechnology, China) and ELISA kits (Sangon Biotech, Shanghai, China), respectively, following their manufacturers' protocols. Briefly, the heart supernatant was mixed with 2',7'-dichlorofluorescein (DCFH) diacetate reagent and incubated at 37 °C in the dark. The concentration of TNF- α , MCP-1, intercellular adhesion molecule-1 (ICAM-1, CD54), IL-6 and IL-1 β in the heart was investigated using 100 μg of protein. Samples were analyzed in triplicate at 450 nm using a microplate reader (Varioskan LUX, Thermo Fisher Scientific, USA). Values were calculated on the basis of a standard curve and reported as picograms per milligram of protein.

2.6. Histological analysis

The whole heart fixed in 4% paraformaldehyde was embedded in paraffin and cut into 5 μm longitudinal sections, then stained with hematoxylin & eosin (H&E) and a Masson dye solution set (Servicebio) according to standard procedures. Inflammatory cell images were acquired using a microscope (DM6B, Leica Micro Systems Inc., USA) with 20 \times and 40 \times objectives. The fibrosis area in treated and control groups (at least 7 sections from 3 consecutive slides per mouse) was analyzed using Image-Pro Plus 7.0 software (Media Cybernetics, Rockville, MD, USA).

2.7. Untargeted metabolomics

For heart samples, 10 mg of heart tissue from each mouse (Control group, 6 mice; Treated group, 6 mice) was excised and homogenized in 750 μL of ice-cold methanol/water (4:1, v/v) for 2 min. After

centrifugation (4 °C, 13,000g) for 10 min, the supernatant was collected and dried in a vacuum. Finally, each dried sample was re-dissolved in 100 μL methanol/water (1:1, v/v) and stored at $-80\text{ }^\circ\text{C}$ until LC-MS analysis. The UPLC and MS conditions for metabolomics and data acquisition are in line with our previous studies (Liao et al., 2021; Song et al., 2020) with some modifications. Briefly, an ultimate 3000 ultrahigh-performance liquid chromatograph (Thermo Fisher Scientific) coupled with a Q-Exactive focus Orbitrap mass spectrometer (Thermo Fisher Scientific) was utilized for untargeted metabolomics. The metabolites were separated in an Xbridge BEH Amide column ($2.1\text{ mm} \times 100\text{ mm}$, 1.7 μm , Waters Corporation, Manchester, UK) and detected by mass spectrometry in both positive and negative ionization modes. For the raw metabolomics data, XCMS online was used for data pre-processing. Detailed metabolomics parameters and data analysis can be obtained from the supplementary information section S2.

2.8. Determination of taurine concentration in mice heart and serum

The extraction of taurine from the heart was the same as in the untargeted metabolomics, except for mixing with 50 ng taurine-D4. For serum samples, 50 μL of serum was mixed with 50 ng taurine-D4 and 500 μL of frozen methanol/water (4:1, v/v) to precipitate protein, then centrifuged at 12,000g for 10 min at 4 °C. A volume of 400 μL of supernatant was collected, dried in a gentle nitrogen flow, and reconstituted with 100 μL of methanol/water (1:1, v/v) for taurine determination. For chromatography, the run time was 5 min at a flow rate of 0.4 mL min^{-1} . The mobile phases were H_2O with 0.1% formic acid (A) and acetonitrile with 0.1% formic acid (B). The programmed gradient was set to 0 min, 85% B; 1 min, 85% B; 2 min, 75% B; 3 min, 65% B; 3.5 min, 50% B; 4.5 min, 50% B; 5 min, 85% B. The temperature of the column oven was 40 °C and the injection volume was 2 μL . For mass spectra, the parameters were set as follows: capillary temperature: 320 °C; aux gas heater temperature: 350 °C; aux gas flow rate: 10 arbitrary units; sheath gas flow rate: 30 psi; spray voltage: 3.5 kV in the positive mode. The resolution for precursor ion m/z was set to 35,000 and 126.0219, and the collision energy was ranged from 10 eV to 30 eV in parallel reaction monitoring (PRM) mode.

Matrix-Assisted Laser Desorption/Ionization–Mass Spectrometry Imaging (MALDI–MSI) was applied to further confirm the variation of taurine and distribution in the heart after $PM_{2.5}$ exposure. The procedure used in this study followed that of previous studies (Wu et al., 2019a; Wu et al., 2019b) with minor modifications. Briefly, all images and MS/MS data were acquired on a rapiflex MALDI TOF/TOF Tissue typer (Bruker Doltonics, Germany) operated by flexImaging 5.0 software (Bruker Doltonics, Germany). MALDI MSI was obtained using a smartbeam 3D laser at a repetition rate of up to 10,000 Hz in negative ion mode at a spatial resolution of 50 μm .

2.9. RNA isolation and real-time quantitative polymerase chain reaction

Total RNA isolation, reverse transcription and real-time quantitative polymerase chain reaction (qRT–PCR) were performed as we previously described (Qi et al., 2013). Briefly, total RNA was isolated from the mouse heart with TRIzol reagent (Invitrogen, Carlsbad, CA, USA) and was reverse-transcribed using cDNA kit according to the manufacturer's instruction (TOYOBO, Japan). The qPCR analysis was conducted on the CFX Connect™ Real-Time PCR Detection System (Bio-Rad) using the MonAmp™ chemoHS qPCR mix (Monad, China). Primer sequences used for each gene are listed in supporting Table S1. The expression was determined by the $2^{-\Delta\Delta CT}$ method using GAPDH as the housekeeping gene.

2.10. Western blot analysis

The total protein extraction from hearts of multi-aged mice is described in the supporting information S3 and protein concentration was determined by Bradford assay with BSA as the standard. The western

blot was performed as we previously described (Qi et al., 2019a). Briefly, the mass of total proteins used in the western blot was 50 µg and Anti-p53 antibody (CST) was used at 1:1000; Anti-β-Actin antibody (CST) was used at 1:1000, Anti-TAUT(A-11) antibody (SANTA CRUZ BIOTECHNOLOGY,INC) was used at 1:250. HRP conjugated Goat Anti-Rabbit IgG and HRP conjugated Goat Anti-Mouse IgG (Servicebio, Wuhan, China) were used at 1:3000 and 1:4000 respectively. Protein signals were developed using a Western Lightening Substrate (Tanon, Shanghai, China) and detected by a JS-1080P Chemiluminescence gel imaging system (Peiqing, Shanghai, China).

2.11. Data analysis

The results are expressed as mean ± SD and were analyzed using GraphPad Prism 7.0 (GraphPad Software, Inc., San Diego, CA). Statistical significance between two groups of means was determined using unpaired Student's *t*-test. Statistical significance between three or more

groups of means was determined using analysis of variance (ANOVA). *P* < 0.05 was considered to be statistically significant.

3. Results and discussion

3.1. Concentration and chemical composition of PM_{2.5}

The mice of different ages were exposed to PM_{2.5} in the real-ambient PM_{2.5} exposure system, where the PM_{2.5} samples were obtained directly from the ambient atmosphere. Therefore, the concentration, components and morphology of PM_{2.5} collected at the exposure site during the study period were first recorded and analyzed. As shown in Fig. 2a, the average daily PM_{2.5} mass concentration in ambient air during the sampling period was 76.8 µg·m⁻³, which is about three times higher than the 25 µg·m⁻³ daily average concentration limit given by the World Health Organization (WHO). In our study, the exposure period was during the hot season in Taiyuan, which is when the highest levels of PM_{2.5} contamination occur

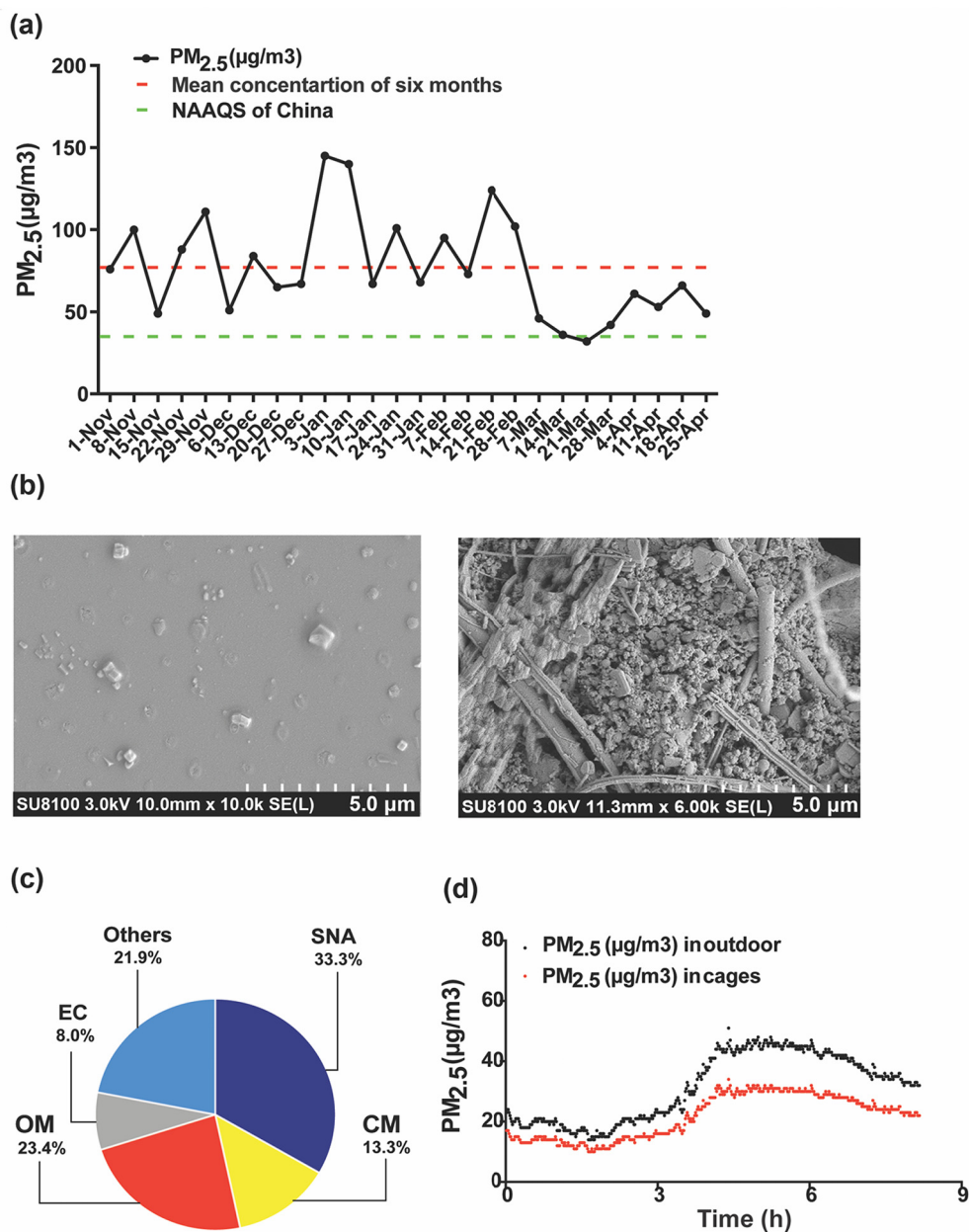


Fig. 2. The characteristics of PM_{2.5} particles at the exposure site during the study period. (a) the mass concentration of ambient PM_{2.5}, (b) the morphology of PM_{2.5} particles, Left: PM_{2.5} in suspension, Right: PM_{2.5} on the filter, Scale bars represent 5 µm, (c) the major chemical components of PM_{2.5} particles, (d) The variation in PM_{2.5} mass concentration in the exposure cages and ambient air.

in the whole year. According to our previous data, the mean concentrations of $PM_{2.5}$ in Taiyuan during the hot period were 98 and $80 \mu\text{g}\cdot\text{m}^{-3}$ in 2016 and 2017, respectively (Zhang et al., 2019; Chen et al., 2020). Although the $PM_{2.5}$ contamination has reduced year on year, the $76.8 \mu\text{g}\cdot\text{m}^{-3}$ $PM_{2.5}$ concentration between November 1, 2018 and April 19, 2019 could still have adverse effects on human health (Qi et al., 2020). The morphology of $PM_{2.5}$ particles suspended in ethanol and attached to the filter was detected by SEM and the results revealed flaky, spherical, quadrate and irregular shaped particles (Fig. 2b), with huge variations in size from 0.06 to 1.2 μm . The major chemical components of $PM_{2.5}$ collected from the exposure site were 33.3% sulfate, nitrate, and ammonium (SNA), 23.4% organic matter (OM), 8% elemental carbon (EC) and 13.3% crustal elements (CM) (Fig. 2c).

Apart from concentration, composition is another vital factor related to the adverse effects of $PM_{2.5}$. In our study, the SNA and OM accounted for more than 50% of the total mass of $PM_{2.5}$ and they are considered to be more toxic than the other constituents (Schlesinger, 2007; Qi et al., 2020). At the same time, the $PM_{2.5}$ concentration in the real-ambient

$PM_{2.5}$ exposure system was also examined to compare the difference between the exposure chamber and the ambient air. Fig. 2d shows that the mass concentration in the exposure cages was lower than that in ambient air, approximately 77% of the level in ambient air. However, the changing trends of $PM_{2.5}$ concentration in the exposure cages and ambient air were consistent. In addition, the $PM_{2.5}$ concentration in the filtered cages was lower than the detection limitations of the machine, which indicated that the $PM_{2.5}$ in the control treatment had been removed.

3.2. $PM_{2.5}$ exposure increased the heart rate of aged mice

HR, the number of times the heart beats per minute, is an accepted indicator for cardiac function. Although normal heart rate varies from person to person and for the same person in different situations, a long-term and stable irregular HR could indicate heart dysfunction. In this study, we traced the changes in HR of mice of different ages in the control and exposure groups. Our results showed that the HR of mice slightly decreased with age, but not significantly, in the control (clean air) group (Fig. 3),

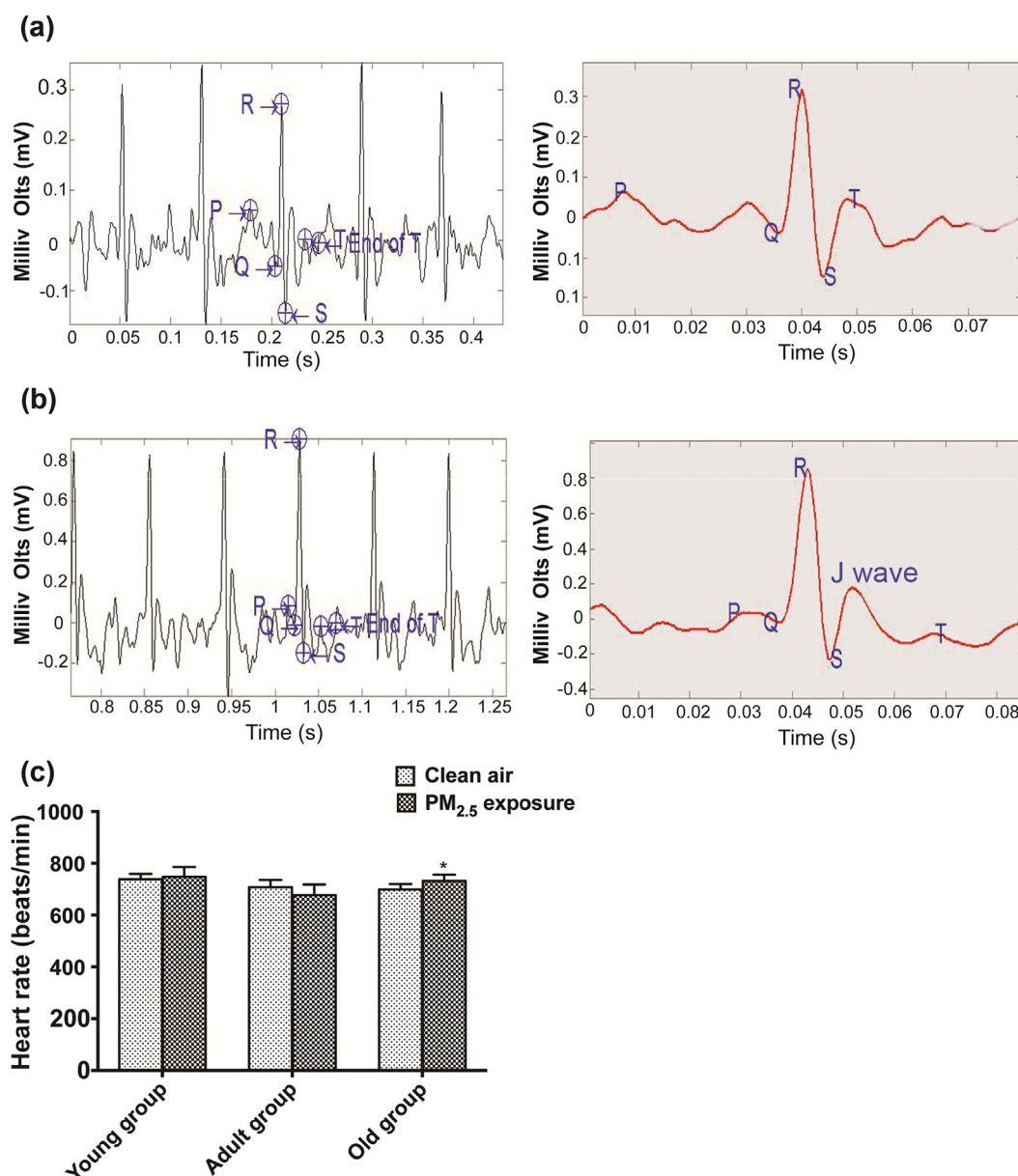


Fig. 3. $PM_{2.5}$ exposure increased the heart rate of aged mice. (a) and (b) Raw traces showing the ECG pattern under basal conditions (Upper) or upon treatment with $PM_{2.5}$ (Lower) in aged mice, (c) heart rate of mice of different ages in the control and exposure groups. Values are mean \pm SD of six mice. * $P < 0.05$.

which is consistent with previous reports that HR is not affected by age in men and women (Lakatta and Levy, 2003). However, exposure of aged mice to PM_{2.5} for 26 weeks clearly increased the heart rate compared to the control group. A clear difference in heart rate between the control and exposure groups could not be found in young and adult mice. At the same time, the body weight, blood pressure and blood glucose also recorded weekly and no significant differences were found between PM_{2.5} exposure and clean air (Fig. S1). Short-term exposure to PM_{2.5} has been proved to be closely associated with the heart rate in humans and animals, with no age-dependent differences (Pei et al., 2016; Rizza et al., 2019). In our study, the abnormal HR induced by chronic PM_{2.5} exposure just occurred in the aged group, which can be explained by the reduced self-repair ability in the aged population. Aging is a major risk factor for cardiovascular diseases, not only because it impairs various processes in the body, but also owing to intrinsic cardiac aging, which reduces cardiac functional reserve, predisposes the heart to stress and

contributes to increased cardiovascular mortality in the elderly. Wang et al. summarized a few epidemiological studies and indicated that the elderly appear particularly susceptible to adverse cardiovascular effects triggered by PM_{2.5} exposure (Wang et al., 2015a). In addition, the HR in obese mice and spontaneously hypertensive rats could also be increased by PM_{2.5} exposure, indicating that the HR in the high cardiovascular disease risk population, is more sensitive to PM_{2.5} exposure (Chang et al., 2004; Song et al., 2020).

3.3. PM_{2.5} exposure induced cardiac oxidative stress, inflammation and fibrosis in aged mice

To investigate further the adverse effects of PM_{2.5} on the hearts of aged mice, oxidative stress, inflammation and fibrosis were examined after aged exposure to PM_{2.5}. The cardiac ROS level caused by PM_{2.5} exposure in aged mice was measured by DCF fluorescence assay. Fig. 4a shows

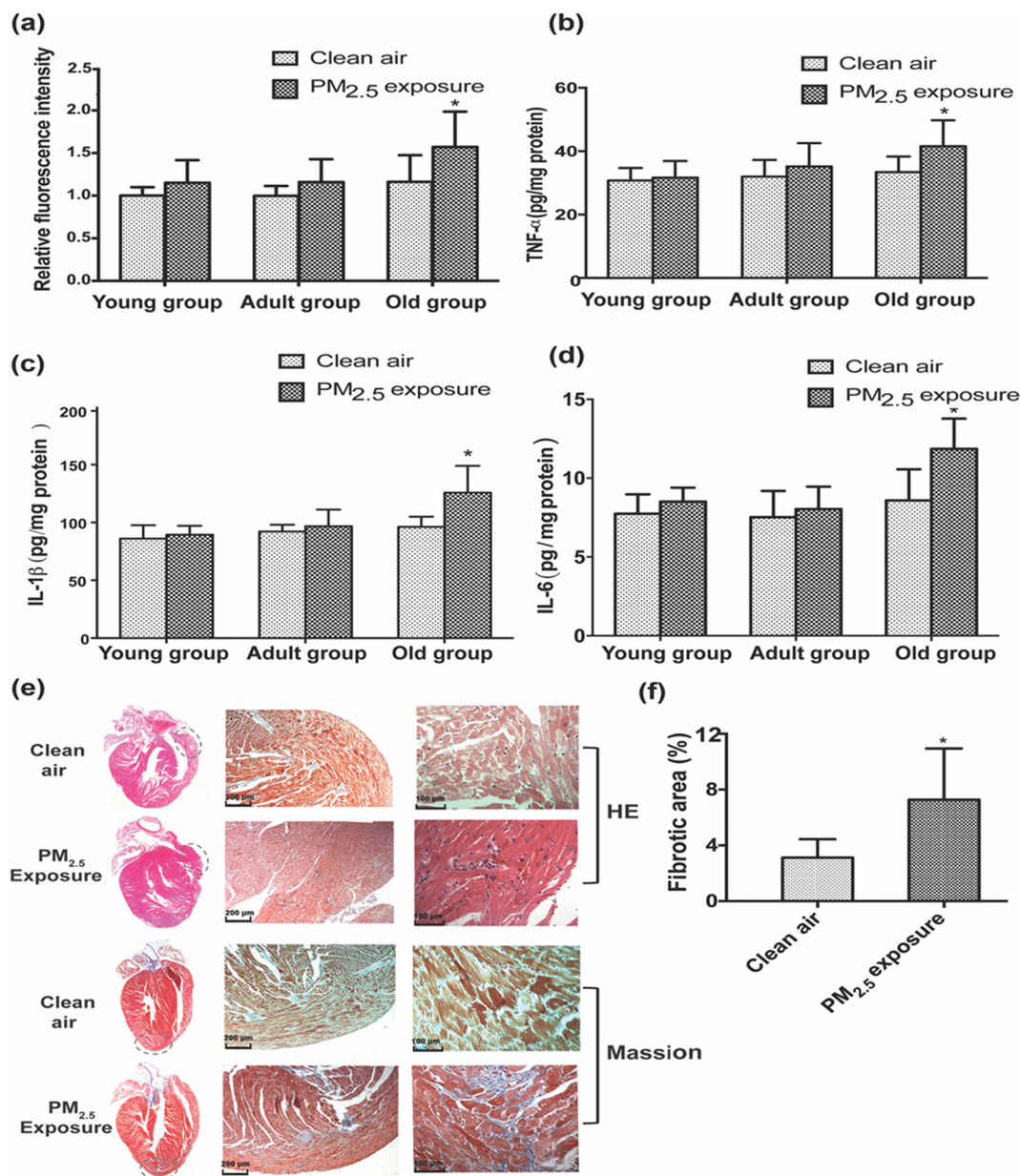


Fig. 4. ROS production, inflammation and fibrosis after chronic PM_{2.5} exposure in aged mice. (a) The ROS intracellular concentration in the hearts of mice of different ages in the clean air and PM_{2.5} exposure groups; (b) (c) (d) The expression level of cytokines (TNF-α, IL-1β and IL-6) in the hearts from clean air and PM_{2.5} exposure groups; Values are mean ± SD of six different mice. *P < 0.05 Vs control group. (e) Representative histopathological images of the hearts of aged mice from the clean air and PM_{2.5} exposure groups (magnification 200×, 400×). (f) The percent of the positive area by Masson's trichrome staining was quantified. Mean ± SD, *P < 0.05 Vs control group.

that there was a clear increase in ROS level in the old group after long-term $PM_{2.5}$ exposure and no significant differences in the young and adult groups. In addition, exposure to $PM_{2.5}$ in aged mice caused a remarkable upregulation in the production of TNF- α , IL-1 β and IL-6 compared with the clean air group (Fig. 4b-d). Moreover, the results of H&E staining and blood routine examination revealed inflammatory cell infiltration, which further confirmed the induction of inflammation after $PM_{2.5}$ exposure in aged mice (Fig. 4e, Table S2). At the same time, the heart of aged mice developed significantly more LV fibrosis after $PM_{2.5}$ exposure than that in the clean air group (Fig. 4e, f).

Numerous experimental and epidemiological studies have shown that the total toxicity of $PM_{2.5}$ is caused by various components of $PM_{2.5}$ which have been implicated in the pathogenesis of several major CVDs (Qi et al., 2020). Oxidative stress and inflammation are the typical toxicological effects induced by $PM_{2.5}$ in organisms. In our study, "real time" exposure of mice to $PM_{2.5}$ (average concentration: $59.1 \mu\text{g} \cdot \text{m}^{-3}$) also induced cardiac oxidative stress and inflammation,

however, this only happened in the old group. We failed to detect excessive oxidative stress and inflammation induced by $PM_{2.5}$ in the hearts of young and adult mice. Therefore, our results for young and adult mice do not support previous findings that $PM_{2.5}$ causes cardiac oxidative stress and inflammation (Duan et al., 2019; Li et al., 2019). These differences can be explained in part by the different $PM_{2.5}$ exposure methods, concentration and components of $PM_{2.5}$. Together with $PM_{2.5}$ toxicology research in obese mice (Song et al., 2020), apolipoprotein E knockout mice (Pei et al., 2016) and AMP sensitive protein kinase knockout mice (Wang et al., 2018), our experiment indicates that the CVD-susceptible population is more sensitive to $PM_{2.5}$ exposure, inducing cardiac oxidative stress and inflammation. According to previous studies, aging is associated with increased levels of ROS and chronic inflammation, decreased immune function and oxidation resistance, which could explain why the cardiac injury was detected only in the old group after chronic exposure (Grimble, 2003; El Assar et al., 2013; Wu et al., 2014).

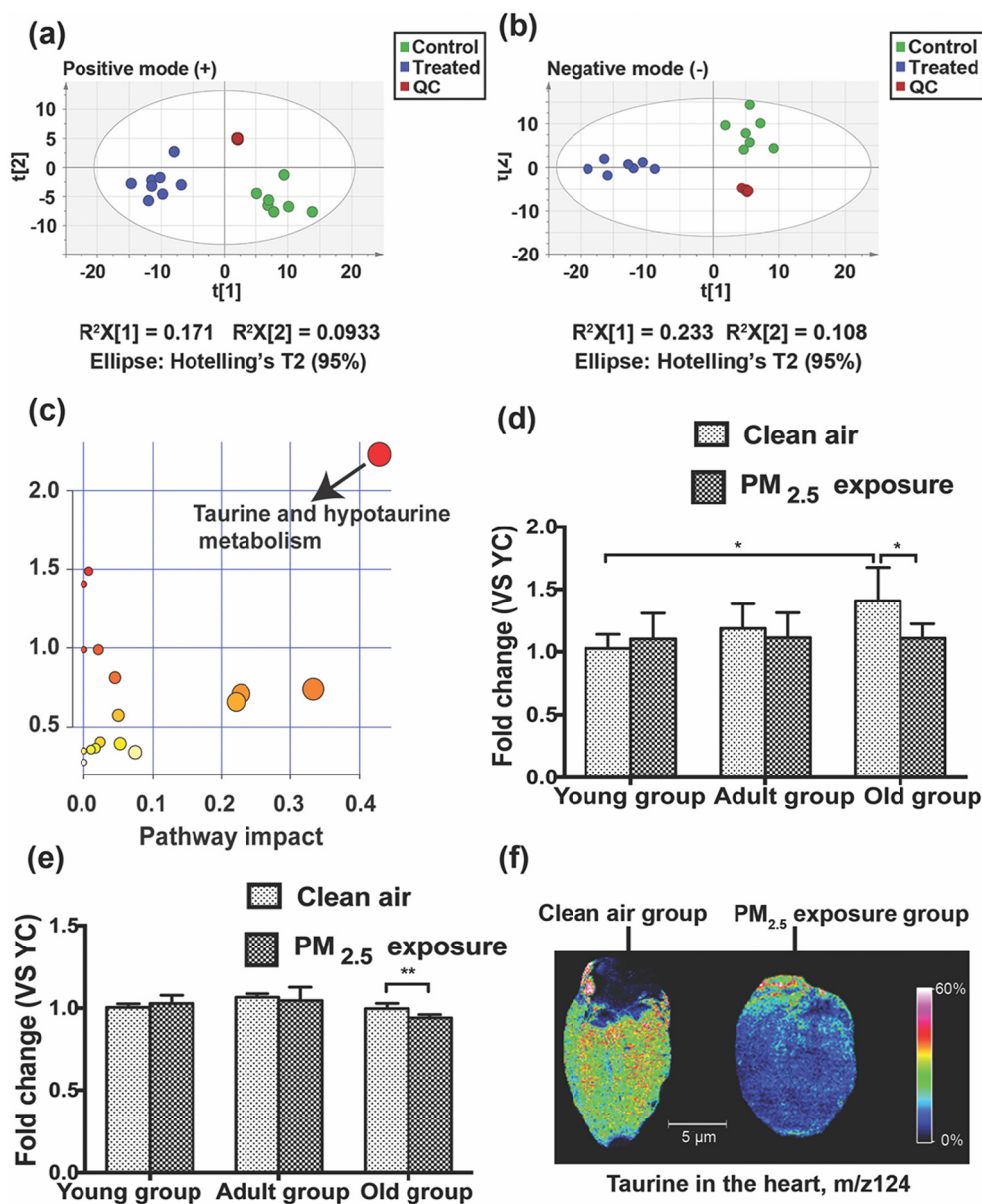


Fig. 5. Untargeted metabolomics analysis of hearts of aged mice and determination of taurine in serum and heart tissue. (a) and (b) The PLS-DA two-dimensional scoring chart of heart tissue in positive mode and negative mode. (c) Pathway analysis of metabolomics. (d) and (e) Determination of taurine in serum and heart tissue of different groups. (f) The MALDI-MSI results for taurine in aged mice hearts in clean air and $PM_{2.5}$ exposure groups. The spatial resolution is $200 \mu\text{m}$ (scale bar, $5 \mu\text{m}$). * $P < 0.05$, ** $P < 0.01$.

3.4. Untargeted metabolomics analysis and source analysis of cardiac taurine

In order to study the toxicity mechanism of PM_{2.5} to the cardiovascular system of aged mice, we performed a non-targeted metabolomics analysis on the heart tissue. After collecting raw data with UPLC-QE-Orbitrap-MS, XCMS online was used for peak alignment, peak grouping and filling gaps of mass spectrometry data to obtain 8504 (4940 in positive mode and 3564 in negative mode) characteristic fragment ions. These fragment ions included important and irrelevant metabolites and signals that could be considered noise, so strict statistical analysis was necessary. From the two-dimensional scoring chart of the partial least squares discrimination analysis (PLS-DA), it can be seen that the data points of the three groups (Control, Treated and QC groups) are clearly separated (Fig. 5a, b), which indicates that PM_{2.5} exposure has a serious impact on the heart metabolism of aged mice. Furthermore, orthogonal partial least squares analysis (OPLS-DA) and *t*-tests were performed on the data for the control group and the treatment group, with VIP > 1 and *P*-value < 0.05 as the screening conditions, and 31 metabolites with significant differences were identified (Table 1).

Through the analysis of the KEGG pathway of the above-mentioned metabolites, it was found that four pathways in the heart tissue of old mice were affected by PM_{2.5}, and the influence on taurine and hypotaurine metabolism was particularly obvious (Fig. 5c). Taurine is a natural amino acid that exists in many mammalian tissues in a free state (De Luca et al., 2015). The source of taurine in the heart of rodents is mainly synthesis in the liver and intake of external food (Huxtable, 2000), which then enters the heart through blood circulation. Therefore, hearts and serum of multi-aged mice (*N* = 3, *n* = 6; young mice: 6 months old; middle-aged mice: 12 months old; aged mice: 17 months old) were used for taurine extraction and semi-quantitative detection (Fig. S2). Before extraction, a known amount of taurine-D4 was added as an internal standard for recovery. The results showed that the

recovery rates of the standard addition were between 60% and 140% (Fig. S3), indicating that the extraction method is appropriate.

Fig. 5d shows that as age increases, the average taurine content in the serum of mice increases, which is consistent with the results of previous work (Wojcik et al., 2013). The concentration of taurine in the heart of middle-aged mice is the highest among the three age groups, while the concentrations of the other two groups are very similar (Fig. 5e). However, after exposure to PM_{2.5}, the concentration of taurine in aged mice decreased significantly in both serum and heart. Based on MALDI-MSI findings, the signal intensities of taurine in the heart were significantly weaker than that of the control group after chronic PM_{2.5} exposure in aged mice (Fig. 5f). In addition, in the hearts of aged mice in the treatment group, taurocholic acid, a metabolite of taurine, a common bile acid with anti-inflammatory and immunomodulatory effects (Wang et al., 2013), also exhibited a sharp decrease in concentration. Therefore, PM_{2.5} may affect the transport of taurine in aged mice, which leads to the lack of taurine in the heart and affects normal physiological functions.

3.5. The effects of PM_{2.5} exposure on the expression level of the taurine transporter in aged mice

The taurine content in the heart not only depends on the taurine concentration in serum but also the expression and activity of TAUT. We next examined the expression level of TAUT and p53 (the potential inhibitor of gene transcription) by western blot analysis. As shown in Fig. 6, there was no significant difference in the expression of TAUT between mice of different ages in the clean air group, which indicated that the expression level in the heart during growth was quite stable. However, chronic PM_{2.5} exposure significantly decreased the expression of TAUT in aged mice (Fig. 6). Zhang et al. reported that taurine content and TAUT expression levels were significantly decreased when cardiomyocytes and cardiac tissues were subjected to adverse

Table 1

The identified metabolites in heart tissue of aged mice.

Compound	mz	RT (min)	HMDB ID	Database	m/z match score	Ions mode	VIP	P-value	Fold change (treated/control)
Cytosine	112.0505	1.05	HMDB0000630	Mona database	1.0000	Positive	1.18	*	0.74
Uracil	113.0346	1.10	HMDB0000300	Mona database	1.0000	Positive	1.79	***	0.59
Taurine	126.0219	8.80	HMDB0000251	Mona database	1.0000	Positive	1.23	*	0.70
N-acetyl-L-alanine	132.0655	0.95	HMDB0000766	Orbitrap database	1.0000	Positive	2.68	****	0.38
3-Dehydroxycarnitine	146.1176	1.01	HMDB06831	HMDB database	1.0000	Positive	1.57	****	1.34
L-histidine	156.0768	1.12	HMDB0000177	Mona database	1.0000	Positive	1.60	****	1.37
L-Carnitine	162.1124	0.97	HMDB0000062	Mona database	0.9999	Positive	1.07	*	1.22
Pantothenic acid	220.1179	4.94	HMDB0000210	Mona database	1.0000	Positive	1.34	***	1.22
Cytidine	244.0928	1.05	HMDB0000089	Mona database	1.0000	Positive	1.09	*	0.72
3-Hydroxyisovalerylcarnitine	262.1649	4.17	HMDB0061189	Orbitrap database	1.0000	Positive	1.65	****	1.46
Nandrolone	275.2005	13.10	HMDB0002725	Mona database	0.9998	Positive	1.77	****	1.55
9-OxoODE	277.2162	16.46	HMDB0004669	Orbitrap database	1.0000	Positive	1.08	*	1.26
Alpha-linolenic acid	279.2318	16.44	HMDB0001388	Mona database	0.9999	Positive	2.44	****	2.10
9-HOTE	295.2267	16.46	HMDB0010224	Mona database	1.0000	Positive	1.20	**	1.26
Dihomo-alpha-linolenic acid	307.2631	17.50	HMDB000039	Orbitrap database	1.0000	Positive	1.61	*	0.59
5,6-Epoxy-8,11,14-eicosatrienoic acid	321.2423	16.22	HMDB0002190	Orbitrap database	1.0000	Positive	1.47	*	0.61
20-Hydroxyarachidonic acid	321.2424	16.76	HMDB05998	Orbitrap database	1.0000	Positive	1.38	*	0.67
Docosahexaenoic acid	329.2474	19.32	HMDB0002183	Mona database	0.9999	Positive	1.92	*	0.49
N-oleoylglycine	340.2846	18.39	HMDB13631	Orbitrap database	1.0000	Positive	1.44	***	1.48
S-adenosylmethionine	399.1444	0.93	HMDB0001185	Mona database	0.9999	Positive	1.08	*	1.16
LysoPC(18:1(9Z)/0:0)	522.3557	15.73	HMDB0002815	Orbitrap database	0.9997	Positive	1.50	***	1.34
LysoPC(18:0/0:0)	524.3714	17.06	HMDB0010384	Orbitrap database	0.9997	Positive	1.38	**	0.68
cis-Aconitic acid	173.0079	1.80	HMDB00072	Orbitrap database	0.9934	Negative	2.36	****	2.42
L-citrulline	174.0872	0.98	HMDB00904	Orbitrap database	0.9932	Negative	1.86	****	1.52
Sebacic acid	201.1124	8.20	HMDB00792	Orbitrap database	0.9965	Negative	1.95	****	1.76
Jasmonic acid	209.1175	11.60	HMDB0032797	Mona database	0.9959	Negative	1.84	****	1.52
9-OxoODE	293.2121	16.46	HMDB0004669	Orbitrap database	1.0000	Negative	2.06	****	1.94
9,10-DHOME	313.2384	15.38	HMDB04704	HMDB database	1.0000	Negative	1.01	*	1.11
N-glycylneuraminic acid	324.0936	0.98	HMDB00833	Orbitrap database	1.0000	Negative	1.58	****	0.59
LysoPE(18:1(9Z)/0:0)	478.2936	16.19	HMDB0011506	Orbitrap database	0.9996	Negative	1.73	***	1.59
Taurocholic acid	514.2841	9.17	HMDB0000036	Mona database	0.9994	Negative	2.69	****	0.23

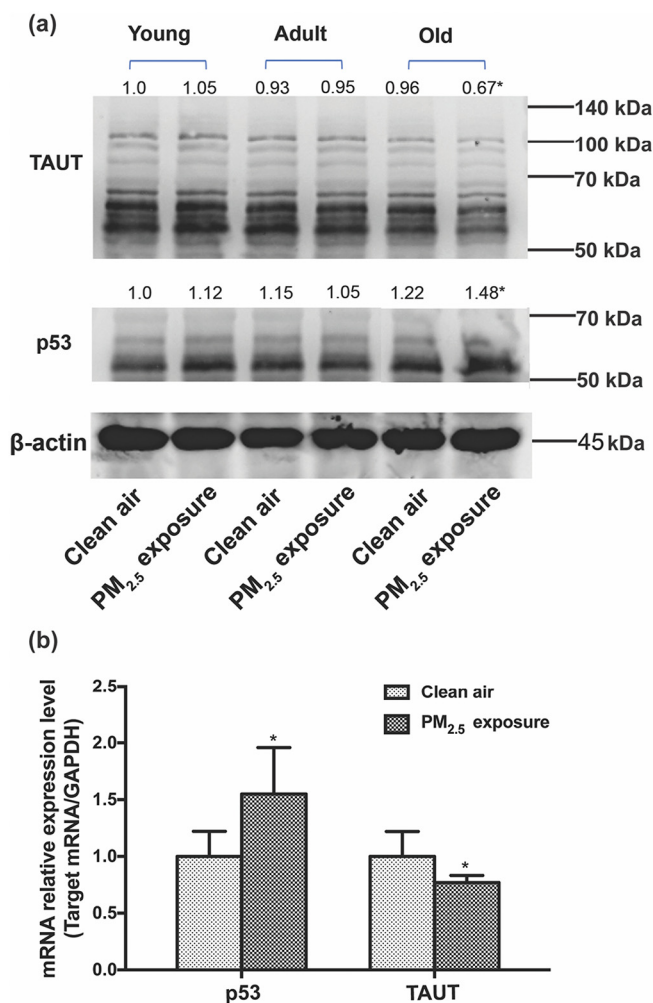


Fig. 6. The effects of PM_{2.5} exposure on the expression level of the TAUT and p53 in aged mice. (a) Western blot analysis of the expression of TAUT and p53 in the mouse hearts after exposure to PM_{2.5} and control. The fold change was normalized against β -tubulin and compared to the control. (b) mRNA expression level of TAUT and p53 in aged mice after exposure to PM_{2.5} and control. GAPDH was used as the internal control. The values are the mean \pm SD of six mice. * $p < 0.05$ versus the control group.

environments such as hypoxic or ischemic stress (Zhang et al., 2013). Therefore, we deduce that TAUT may be an important effect target of the cardiovascular system when exposed to internal and external stress. The TAUT gene transcription was down-regulated by p53 and the binding sites of p53 located in the promoter region of the TAUT gene (Han et al., 2002). In our study, the expressions of p53 in all treatment and control groups were examined and we found remarkable elevation in the hearts of aged mice after chronic exposure; however, no significant differences were found between treatment and control groups for young and adult mice, indicating that the reduction in TAUT might be attributed to the PM_{2.5}-induced p53 activation.

Several lines of evidence showed p53, as the “guardian of genome”, plays various roles in the defense mechanisms for cellular adverse outcomes, such as DNA damage, senescence and apoptosis and also can be activated by ROS, especially during chronic inflammation (Shi and Dansen, 2020). Experimental studies using in vitro and in vivo models have emphasized the roles of p53 in PM_{2.5} induced cardiomyocytes apoptosis and cardiac dysfunction (Wang et al., 2019; Yang et al., 2019). Based on the above results, it can be speculated that the expression of TAUT may be negatively regulated by excessive ROS production and p53 activation induced directly or indirectly by chronic PM_{2.5} exposure in aged mice, which contributed to the reduction of cardiac taurine.

Remarkably, the downregulation of cardiac taurine could cause and further exacerbate heart dysfunction due to its vital role in maintaining the heart function.

4. Conclusions

The purpose of the current study was to determine the age-dependent effects of PM_{2.5} on the cardiovascular system and the mechanisms underlying the effects of chronic exposure of PM_{2.5}. The chemical and physical properties of PM_{2.5} used in the exposure system indicated the higher exposure risk due to the high concentration of PM_{2.5} and the presence of numerous toxic components. Our research has also shown that chronic PM_{2.5} exposure mostly affected the heart function of aged mice rather than that of young and adult groups. Untargeted metabolomics and biotechnology analysis suggested that taurine reduction, which was caused by the decreased serum taurine level and the expression and activity of TAUT, was associated with heart dysfunction induced by chronic PM_{2.5} exposure. In summary, our current study reveals the importance of taurine as the novel cardiac effect target for PM_{2.5}-induced heart dysfunction in the aged group.

Declaration of competing interest

The authors declare no conflict of interest with respect to the study or preparation of the manuscript.

Acknowledgements

This work was supported by the National Natural Science Foundation of China (21806025 and 91843301), the Natural Science Foundation of Guangdong Province (2019A1515011294), Science and Technology Planning Project of Guangdong Province (2020B1212030008), National Key Research and Development Project (2019YFC1804604).

Appendix A. Supplementary data

Figs. S1–S6, Tables S1, S2 and supporting methods S1–S3 are available in the Supporting Information, which is free of charge via the Internet. Supplementary data to this article can be found online at <https://doi.org/10.1016/j.scitotenv.2021.146866>.

References

- Baliou, S., Kyriakopoulos, A.M., Goulielmaki, M., Panayiotidis, M.I., Spandidos, D.A., Zoumpourlis, V., 2020. Significance of taurine transporter (TauT) in homeostasis and its layers of regulation (review). *Mol. Med. Rep.* 22, 2163–2173.
- Bastiaansen, M., Ait Bamai, Y., Araki, A., Van den Eede, N., Kawai, T., Tsuboi, T., Kishi, R., Covaci, A., 2019. Biomonitoring of organophosphate flame retardants and plasticizers in children: associations with house dust and housing characteristics in Japan. *Environ. Res.* 172, 543–551.
- Chang, C.C., Hwang, J.S., Chan, C.C., Wang, P.Y., Hu, T.H., Cheng, T.J., 2004. Effects of concentrated ambient particles on heart rate, blood pressure, and cardiac contractility in spontaneously hypertensive rats. *Inhal. Toxicol.* 16, 421–429.
- Chen, Y.Y., Song, Y.Y., Chen, Y.J., Zhang, Y.H., Li, R.J., Wang, Y.J., Qi, Z.H., Chen, Z.F., Cai, Z.W., 2020. Contamination profiles and potential health risks of organophosphate flame retardants in PM_{2.5} from Guangzhou and Taiyuan, China. *Environ. Int.* 134, 105343.
- Dawson, R., Eppler, B., Patterson, T.A., Shih, D., Liu, S., 1996. The effects of taurine in a rodent model of aging. *Taurine* 2. Springer, pp. 37–50.
- De Luca, A., Piermo, S., Camerino, D.C., 2015. Taurine: the appeal of a safe amino acid for skeletal muscle disorders. *J. Transl. Med.* 13.
- Duan, S., Wang, N., Huang, L., Zhao, Y., Shao, H., Jin, Y., Zhang, R., Li, C., Wu, W., Wang, J., Feng, F., 2019. NLRP3 inflammasome activation is associated with PM_{2.5}-induced cardiac functional and pathological injury in mice. *Environ. Toxicol.* 34, 1246–1254.
- El Assar, M., Angulo, J., Rodriguez-Manas, L., 2013. Oxidative stress and vascular inflammation in aging. *Free Radic. Biol. Med.* 65, 380–401.
- Grimble, R.F., 2003. Inflammatory response in the elderly. *Curr. Opin. Clin. Nutr. Metab. Care* 6, 21–29.
- Han, X.B., Patters, A.B., Chesney, R.W., 2002. Transcriptional repression of taurine transporter gene (TauT) by p53 in renal cells. *J. Biol. Chem.* 277, 39266–39273.
- Heuermann, R.J., Jaramillo, T.C., Ying, S.W., Suter, B.A., Lyman, K.A., Han, Y., Lewis, A.S., Hampton, T.G., Shepherd, G.M.G., Goldstein, P.A., Chetkovich, D.M., 2016. Reduction

- of thalamic and cortical I-h by deletion of TRIP8b produces a mouse model of human absence epilepsy. *Neurobiol. Dis.* 85, 81–92.
- Huxtable, R.J., 2000. Expanding the circle 1975–1999: sulfur biochemistry and insights on the biological functions of taurine. *Adv. Exp. Med. Biol.* 483, 1–25.
- Jia, Y.Y., Wang, Q., Liu, T., 2017. Toxicity research of PM_{2.5} compositions in vitro. *Int. J. Environ. Res. Public Health* 14.
- Kan, H.D., Chen, B.H., Zhao, N.Q., London, S.J., Song, G.X., Chen, G.H., Zhang, Y.H., Jiang, L.L., Committee, H.E.I.H.R., 2010. Part 1. A time-series study of ambient air pollution and daily mortality in Shanghai, China. *Res Rep Health Eff Inst.* pp. 17–78.
- Lakatta, E.G., Levy, D., 2003. Arterial and cardiac aging: major shareholders in cardiovascular disease enterprises: part II: the aging heart in health: links to heart disease. *Circulation* 107, 346–354.
- Li, R.J., Kou, X.J., Geng, H., Xie, J.F., Tian, J.F., Cai, Z.W., Dong, C., 2015. Mitochondrial damage: an important mechanism of ambient PM_{2.5} exposure-induced acute heart injury in rats. *J. Hazard. Mater.* 287, 392–401.
- Li, D.C., Zhang, R., Cui, L.H., Chu, C., Zhang, H.Y., Sun, H., Luo, J., Zhou, L.X., Chen, L.P., Cui, J., Chen, S., Mai, B.X., Chen, S.J., Yu, J.Z., Cai, Z.W., Zhang, J.Q., Jiang, Y.S., Aschner, M., Chen, R., Zheng, Y.X., Chen, W., 2019. Multiple organ injury in male C57BL/6j mice exposed to ambient particulate matter in a real-ambient PM exposure system in Shijiazhuang, China. *Environ. Pollut.* 248, 874–887.
- Liao, X.L., Zou, T., Chen, M., Song, Y.Y., Yang, C., Qiu, B.J., Chen, Z.F., Tsang, S.Y., Qi, Z.H., Cai, Z.W., 2021. Contamination profiles and health impact of benzothiazole and its derivatives in PM_{2.5} in typical Chinese cities. *Sci. Total Environ.* 755, 142617.
- Liu, C., Chen, R.J., Sera, F., Vicedo-Cabrera, A.M., Guo, Y.M., Tong, S.L., Coelho, M., Saldiva, P.H.N., Lavigne, E., Matus, P., Valdes Ortega, N., Osorio Garcia, S., Pascal, M., Stafoggia, M., Scortichini, M., Hashizume, M., Honda, Y., Hurtado-Díaz, M., Cruz, J., Nunes, B., Teixeira, J.P., Kim, H., Tobias, A., Iñiguez, C., Forsberg, B., Åström, C., Ragettli, M.S., Guo, Y.L., Chen, B.Y., Bell, M.L., Wright, C.Y., Scovronick, N., Garland, R.M., Milojevic, A., Kysej, J., Urban, A., Orru, H., Indermitte, E., Jaakkola, J.J.K., Rytö, N.R.I., Katsouyanni, K., Analitis, A., Zanobetti, A., Schwartz, J., Chen, J.M., Wu, T.C., Cohen, A., Gasparrini, A., Kan, H.D., 2019. Ambient particulate air pollution and daily mortality in 652 cities. *N. Engl. J. Med.* 381, 705–715.
- Luo, Q., Cai, Z.W., Wong, M.H., 2007. Polybrominated diphenyl ethers in fish and sediment from river polluted by electronic waste. *Sci. Total Environ.* 383, 115–127.
- Miao, Y.C., Liu, S.H., Guo, J.P., Yan, Y., Huang, S.X., Zhang, G., Zhang, Y., Lou, M.Y., 2018. Impacts of meteorological conditions on wintertime PM(2.5) pollution in Taiyuan, North China. *Environ. Sci. Pollut. Res. Int.* 25, 21855–21866.
- Pei, Y.L., Jiang, R.F., Zou, Y.Z., Wang, Y., Zhang, S.H., Wang, G.H., Zhao, J.Z., Song, W.M., 2016. Effects of fine particulate matter (PM_{2.5}) on systemic oxidative stress and cardiac function in ApoE(–/–) mice. *Int. J. Environ. Res. Public Health* 13.
- Pozzi, R., De Berardis, B., Paoletti, L., Guastadisegni, C., 2003. Inflammatory mediators induced by coarse (PM_{2.5-10}) and fine (PM_{2.5}) urban air particles in RAW 264.7 cells. *Toxicology* 183, 243–254.
- Pun, V.C., Kazemparkouhi, F., Manjourides, J., Suh, H.H., 2017. Long-term PM_{2.5} exposure and respiratory, cancer, and cardiovascular mortality in older US adults. *Am. J. Epidemiol.* 186, 961–969.
- Qi, Z.H., Liu, Y.F., Luo, S.W., Chen, C.X., Liu, Y., Wang, W.N., 2013. Molecular cloning, characterization and expression analysis of tumor suppressor protein p53 from orange-spotted grouper, *Epinephelus coioides* in response to temperature stress. *Fish Shellfish Immunol.* 35, 1466–1476.
- Qi, Z.H., Chen, M., Song, Y.Y., Wang, X.Y., Li, B.K., Chen, Z.F., Tsang, S.Y., Cai, Z.W., 2019a. Acute exposure to triphenyl phosphite inhibits the proliferation and cardiac differentiation of mouse embryonic stem cells and zebrafish embryos. *J. Cell. Physiol.* 234, 21235–21248.
- Qi, Z.H., Song, Y.Y., Ding, Q.Q., Liao, X.L., Li, R.J., Liu, G.G., Tsang, S.Y., Cai, Z.W., 2019b. Water soluble and insoluble components of PM_{2.5} and their functional cardiotoxicities on neonatal rat cardiomyocytes in vitro. *Ecotoxicol. Environ. Saf.* 168, 378–387.
- Qi, Z.H., Zhang, Y.H., Chen, Z.F., Yang, C., Song, Y.Y., Liao, X.L., Li, W.Q., Tsang, S.Y., Liu, G.G., Cai, Z.W., 2020. Chemical identity and cardiovascular toxicity of hydrophobic organic components in PM_{2.5}. *Ecotoxicol. Environ. Saf.* 201, 110827.
- Rizza, V., Stabile, L., Vistocco, D., Russi, A., Pardi, S., Buonanno, G., 2019. Effects of the exposure to ultrafine particles on heart rate in a healthy population. *Sci. Total Environ.* 650, 2403–2410.
- Sacks, J.D., Stanek, L.W., Luben, T.J., Johns, D.O., Buckley, B.J., Brown, J.S., Ross, M., 2011. Particulate matter-induced health effects: who is susceptible? *Environ. Health Perspect.* 119, 446–454.
- Schaffer, S., Kim, H.W., 2018. Effects and mechanisms of taurine as a therapeutic agent. *Biomol. Ther. (Seoul)* 26, 225–241.
- Schlesinger, R.B., 2007. The health impact of common inorganic components of fine particulate matter (PM_{2.5}) in ambient air: a critical review. *Inhal. Toxicol.* 19, 811–832.
- Shi, T., Dansen, T.B., 2020. ROS induced p53 activation: DNA damage, redox signaling or both? *Antioxid. Redox Signal.* 33, 839–859.
- Song, Y.Y., Qi, Z.H., Zhang, Y.H., Wei, J.T., Liao, X.L., Li, R.J., Dong, C., Zhu, L., Yang, Z., Cai, Z.W., 2020. Effects of exposure to ambient fine particulate matter on the heart of diet-induced obesity mouse model. *Sci. Total Environ.* 732, 139304.
- Wang, C.Y., Li, L., Guan, H., Tong, S.Y.N., Liu, M.Q., Liu, C., Zhang, Z.Y., Du, C.G., Li, P.F., 2013. Effects of taurocholic acid on immunoregulation in mice. *Int. Immunopharmacol.* 15, 217–222.
- Wang, C.C., Tu, Y.F., Yu, Z.L., Lu, R.Z., 2015a. PM_{2.5} and cardiovascular diseases in the elderly: an overview. *Int. J. Environ. Res. Public Health* 12, 8187–8197.
- Wang, T., McDonald, C., Petrenko, N.B., Leblanc, M., Wang, T., Giguere, V., Evans, R.M., Patel, V.V., Pei, L.M., 2015b. Estrogen-related receptor α (ERR α) and ERR γ are essential coordinators of cardiac metabolism and function. *Mol. Cell Biol.* 35, 1281–1298.
- Wang, H.Y., Shen, X.Y., Tian, G.X., Shi, X.L., Huang, W., Wu, Y.G., Sun, L., Peng, C., Liu, S.S., Huang, Y., Chen, X.Y., Zhang, F., Chen, Y.J., Ding, W.J., Lu, Z.B., 2018. AMPK α 2 deficiency exacerbates long-term PM_{2.5} exposure-induced lung injury and cardiac dysfunction. *Free Radic. Biol. Med.* 121, 202–214.
- Wang, Q., Gan, X.D., Li, F., Chen, Y., Fu, W.L., Zhu, X.M., Xu, D.Q., Long, M.H., Xu, D.G., 2019. PM(2.5) exposure induces more serious apoptosis of cardiomyocytes mediated by Caspase3 through JNK/P53 pathway in hyperlipidemic rats. *Int. J. Biol. Sci.* 15, 24–33.
- West, J.J., Cohen, A., Dentener, F., Brunekreef, B., Zhu, T., Armstrong, B., Bell, M.L., Brauer, M., Carmichael, G., Costa, D.L., Dockery, D.W., Kleeman, M., Krzyzanowski, M., Kunzli, N., Liousse, C., Lung, S.C.C., Martin, R.V., Poschl, U., Pope, C.A., Roberts, J.M., Russell, A.G., Wiedinmyer, C., 2016. What we breathe impacts our health: improving understanding of the link between air pollution and health. *Environ. Sci. Technol.* 50, 4895–4904.
- Wojcik, O.P., Koenig, K.L., Zeleniuch-Jacquotte, A., Pearte, C., Costa, M., Chen, Y., 2013. Serum taurine and risk of coronary heart disease: a prospective, nested case-control study. *Eur. J. Nutr.* 52, 169–178.
- Wu, J.Z., Xia, S.J., Kalionis, B., Wan, W.B., Sun, T., 2014. The role of oxidative stress and inflammation in cardiovascular aging. *Biomed. Res. Int.* 2014, 615312.
- Wu, H., Dai, Z.F., Liu, X., Lin, M., Gao, Z.Y., Tian, F., Zhao, X., Sun, Y., Pu, X.P., 2019a. Pharmacodynamic evaluation of Shenfu injection in rats with ischemic heart failure and its effect on small molecules using matrix-assisted laser desorption/ionization-mass spectrometry imaging. *Front. Pharmacol.* 10, 1424.
- Wu, H., Liu, X., Gao, Z.Y., Dai, Z.F., Lin, M., Tian, F., Zhao, X., Sun, Y., Pu, X.P., 2019b. Anti-myocardial infarction effects of Radix Aconiti Lateralis Preparata extracts and their influence on small molecules in the heart using matrix-assisted laser desorption/ionization-mass spectrometry imaging. *Int. J. Mol. Sci.* 20.
- Xu, M.M., Jia, Y.P., Li, G.X., Liu, L.Q., Mo, Y.Z., Jin, X.B., Pan, X.C., 2013. Relationship between ambient fine particles and ventricular repolarization changes and heart rate variability of elderly people with heart disease in Beijing, China. *Biomed. Environ. Sci.* 26, 629–637.
- Xu, Y.Y., Wang, W.J., Zhou, J., Chen, M.J., Huang, X.K., Zhu, Y.N., Xie, X.Y., Li, W.H., Zhang, Y.H., Kan, H.D., Ying, Z.K., 2019. Metabolomics analysis of a mouse model for chronic exposure to ambient PM_{2.5}. *Environ. Pollut.* 247, 953–963.
- Yang, X.Z., Zhao, T., Feng, L., Shi, Y.F., Jiang, J.J., Liang, S., Sun, B.Y., Xu, Q., Duan, J.C., Sun, Z.W., 2019. PM_{2.5}-induced ADRB2 hypermethylation contributed to cardiac dysfunction through cardiomyocytes apoptosis via PI3K/Akt pathway. *Environ. Int.* 127, 601–614.
- Zhang, Y., Yang, L., Yang, Y.J., Liu, X.Y., Jia, J.G., Qian, J.Y., Wang, K.Q., Zuo, J., Ge, J.B., 2013. Low-dose taurine upregulates taurine transporter expression in acute myocardial ischemia. *Int. J. Mol. Med.* 31, 817–824.
- Zhang, H.H., Li, Z., Liu, Y., Xinan, P., Cui, X.Y., Ye, H., Hu, B.L., Lou, L.P., 2018. Physical and chemical characteristics of PM(2.5) and its toxicity to human bronchial cells BEAS-2B in the winter and summer. *J Zhejiang Univ Sci B* 19, 317–326.
- Zhang, Y.H., Chen, Y.Y., Li, R.J., Chen, W., Song, Y.Y., Hu, D., Cai, Z.W., 2019. Determination of PM_{2.5}-bound polyaromatic hydrocarbons and their hydroxylated derivatives by atmospheric pressure gas chromatography-tandem mass spectrometry. *Talanta* 195, 757–763.
- Zhou, M.G., Wang, H.D., Zeng, X.Y., Yin, P., Zhu, J., Chen, W.Q., Li, X.H., Wang, L.J., Wang, L.M., Liu, Y.N., Liu, J.e., Zhang, M., Qi, J.L., Yu, S.C., Afshin, A., Gakidou, E., Glenn, S., Krish, V.S., Miller-Petrie, M.K., Mountjoy-Venning, W.C., Mullany, E.C., Redford, S.B., Liu, H.Y., Naghavi, M., Hay, S.I., Wang, L.H., Murray, C.J.L., Liang, X.F., 2019. Mortality, morbidity, and risk factors in China and its provinces, 1990–2017: a systematic analysis for the Global Burden of Disease Study 2017. *Lancet* 394, 1145–1158.